Inorg. Chem. **2007**, *46*, 11106–11111

Prussian Blue Analogue $CsFe[Cr(CN)_6]$ as a Matrix for the Fe(II) Spin-Crossover

Boris Le Guennic, Serguei Borshch, and Vincent Robert*

Ecole normale supérieure de Lyon, Laboratoire de Chimie, UMR 5182, 46 allée d'Italie, F-69364 Lyon

Received July 9, 2007

The origin of the intriguing spin-transition behavior of the Prussian blue analogue cesium iron hexacyanochromate $CsFe[Cr(CN)_6]$ has been investigated by means of correlated ab initio CASPT2 calculations. Using the smallest transiting core $[Fe(NC)_6]^{4-}$, the relative importance of the local ligand field and the Madelung field generated by the rest of the crystal was estimated. It is shown that in the presence of a frozen-charge environment, the high-spin state lies lower in energy than the low-spin state, thus excluding the possibility of observing a spin transition. In contrast, the charge reorganization in the environment evaluated from unrestricted periodic Hartree–Fock calculations creates a prerequisite for the spin-transition phenomenon. The influence of the disorder in the cesium ions' positions on the spin transition has been examined as a possible stabilizing factor of the low-spin state of $[Fe(NC)_6]^{4-}$. It is concluded that this experimentally observed disorder cannot account solely for the unprecedented behavior of the $CsFe[Cr(CN)_6]$ compound.

Introduction

The family of Prussian blue analogues (PBA) has been widely studied in the field of molecular magnetism.[1] Currently, the interest for these compounds is motivated by two reasons. First, the representatives of this family that contain vanadium and chromium cations behave as high-temperature magnets.[2] Second, some PBA display temperature- and photoinduced magnetic phase transitions.[1c,3] These transitions usually result from temperature or optically driven electron transfer between two metal ions in the lattice. The change of the oxidation states leads to changes in the metal ions spin states, thus inducing or modifying the magnetic coupling between them. The recently observed[4] spin transition at the iron(II) center in the cesium iron hexacyanochromate $CsFe[Cr(CN)_6]$ compound (Figure 1) has opened a new chapter in the applications of PBA in molecular magnetism.

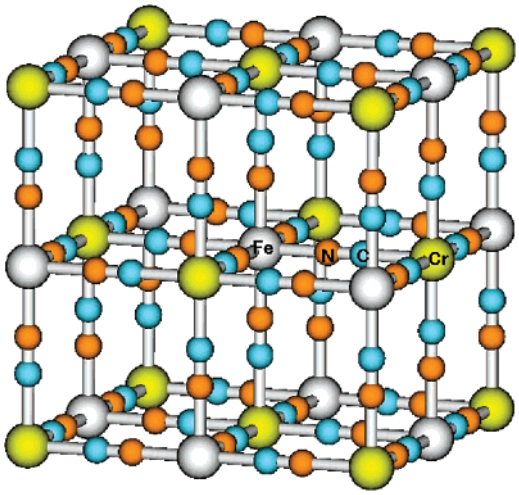

Figure 1. Spin transiting $CsFe[Cr(CN)_6]$ system. Iron, chromium, carbon, and nitrogen atoms are shown in gray, green, blue, and orange, respectively. Cesium ions are omitted.

* To whom correspondence should be addressed. E-mail: vincent.robert@ens-lyon.fr.

(1) For reviews, see (a) Verdaguer, M.; Bleuzen, A.; Marvaud, V.; Vaisserman, J.; Seuleiman, M.; Desplanches, C.; Scuiller, A.; Train, C.; Garde, R.; Gelly, G.; Lomenech, C.; Rosenman, I.; Veillet, P.; Cartier, C.; Villain, F. *Coord. Chem. Rev.* **1999**, *190−192*, 1023−1047. (b) Verdaguer, M.; Girolami, G. S. In *Magnetism: Molecules to Materials V*; Miller, J. S., Drillon, M., Eds.; Wiley-VCH: Weinheim, Germany, 2005; pp 283−346. (c) Ohkoshi, S.; Tokoro, H.; Hashimoto, K. *Coord. Chem. Rev.* **2005**, *249*, 1830−1840.

(2) (a) Ferlay, S.; Mallah, T.; Ouahès, P.; Veillet, P.; Verdaguer, M. *Nature* **1995**, *378*, 701−703. (b) Holmes, S. M.; Girolami, G. S. *J. Amer. Chem. Soc.* **1999**, *121*, 5593−5594. (c) Hatlevik, Ø.; Bushmann, W. E.; Zhang, J.; Manson, J. L.; Miller, J. S. *Adv. Mater.* **1999**, *11*, 914−918.

(3) (a) Sato, O.; Iyoda, T.; Fujishima, A.; Hashimoto, K. *Science* **1996**, *272*, 704−705. (b) Bleuzen, A.; Lomenech, C.; Escax, V.; Villain, F.; Varret, F.; Cartier dit Moulin, C.; Verdaguer, M. *J. Am. Chem. Soc.* **2000**, *122*, 6648−6652.

(4) Kosaka, W.; Nomura, K.; Hashimoto, K.; Ohkoshi, S. *J. Am. Chem. Soc.* **2005**, *127*, 8590−8591.

10.1021/ic701352c CCC: $37.00
Published on Web 11/23/2007

In this compound, the thermal spin transition results from the crossover of the high-spin (HS) and low-spin (LS) states of the iron(II) ions without any intervalence electron transfer in the lattice. This particular observation is very surprising, as the coordination site of a two-valent metal ion [$M^{II}(NC)_6$] (i.e., nitrogen-bonded cyano ligand) undergoes a low or mean ligand field. Thus, a high-spin behavior can be anticipated. This conclusion has been confirmed by high-level ab initio calculations performed on the $[Fe(NCH)_6]^{2+}$ ion.[5] However, for the LS $\leftrightarrow$ HS entropy-driven spin transition to occur, the complex must possess a LS electronic ground state. Because the $[Fe(CN)_6]^{4-}$ complexes are known to be LS, one mechanism for the LS-state stabilization may be found in the cyanide flips in the hexacyano iron(II) units. As a matter of fact, the existence of a spin transition associated with the cyano-group flip (the so-called linkage isomerization) in an iron(II)−chromium(III) PBA has been recently demonstrated in experiments under external pressure.[6] Even though a small number of iron(II) centers with a flipped cyanide ligand is present in the CsFe[Cr(CN)$_6$] crystal lattice, the IR spectra unambiguously indicate that the spin transition takes place in the FeN_6 coordination centers without any isomerization of the iron−cyanide bond.[4] It has been recently shown that the HS to LS transition of the iron(II) centers can be triggered by X-ray illumination as well.[7] The same group has also described a spectacular shift of the spin-transition temperature under external pressure.[8] Therefore, the combination of these experimental studies suggests that the crystal environment in the cesium iron hexacyanochromate CsFe[Cr(CN)$_6$] is likely to introduce some determining factors, leading to the inversion of the $Fe(NC)_6$ unit spin levels ordering as compared to the gas phase. How much the environment may control the LS to HS transition on the iron center is an important question in such PBA. In contrast with commonly studied molecular crystal spin-transition systems, the CsFe[Cr(CN)$_6$] compound is a 3D covalently bonded solid, which makes it a rather intriguing system. Thus, part of the answer is to be found in rigorous calculations on model molecular systems properly embedded into the crystal environment. Along the spin transition, two noticeable degrees of freedom may play a major role, namely the bond distances relaxation and the charge redistribution.

In the present article, we report results of complete active space self-consistent field (CASSCF) and subsequent second-order perturbation theory (CASPT2) calculations. We demonstrate the determining contribution of the charge redistribution in the Madelung field definition. The sensitivity of the spin transition to the local environment was analyzed to rationalize the role of the CsFe[Cr(CN)$_6$] matrix in the spin crossover of the iron(II) centers. By varying independently the geometries of the metal $Fe(NC)_6$ complex and the environment's type and size, the energy gap between the HS $^5T_{2g}$ and LS $^1A_{1g}$ states was estimated. On the basis of this strategy, one can grasp not only the importance upon the spin transition of the local Madelung field but also the short range versus long-range effects. In particular, how much two different sites can coexist in this 3D network is a major issue, which is addressed in the present work. Finally, because the specific role of the alkali ion in the spin transition associated with electron transfer in Prussian Blue derivatives[9] has been considered in the literature, the cesium ion disorder is also investigated in this work as a possible driving force.

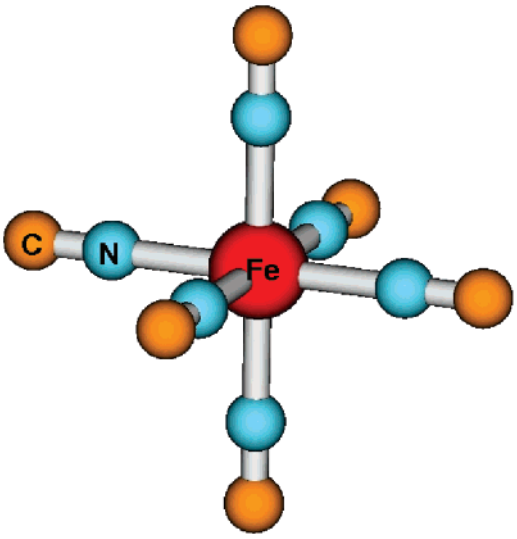

Figure 2. $[Fe(NC)_6]^{4-}$ model complex.

Computational Details

It is known that some care must be taken to properly define the energy spectrum of open-shell systems. Even though density functional theory calculations have the ability to tackle relatively large systems, it has been recently confirmed that some inherent drawbacks to this methodology may lead to unsatisfactory results.[10] In particular, the exact-exchange admixture in the functional is a critical parameter in the description of the spin-states energetics of metal complexes.[11] As demonstrated in numerous works,[12] a spectroscopic accuracy can be reached using CASSCF and CASPT2 calculations. However, extended basis sets combined with rather-large active spaces are necessary to reach this goal.[10] Because we were primarily interested in understanding the driving forces of spin transition, different model clusters can be considered. We focused on the smallest spin transiting unit of our system, namely $[Fe(NC)_6]^{4-}$ (Figure 2).

The structural characteristics of the studied compound in both spin states were taken from ref 7, and we did not perform any geometry optimization. Because the importance of the Madelung

(5) Bolvin, H. *J. Phys. Chem. A* **1998**, *102*, 7525−7534.
(6) Coronado, E.; Giménez-Lopez, M. C.; Levchenko, G.; Romero, F. M.; Garcia-Baonza, V.; Milner, A.; Paz-Pasternak, M. *J. Am. Chem. Soc.* **2005**, *127*, 4580−4581.
(7) Papanikolaou, D.; Margadonna, S.; Kosaka, W.; Ohkoshi, S.; Brunelli, M.; Prassides, K. *J. Am. Chem. Soc.* **2006**, *128*, 8358−8363.
(8) Papanikolaou, D.; Kosaka, W.; Margadonna, S.; Kagi, H.; Ohkoshi, S.; Prassides, K. *J. Phys. Chem. C* **2007**, *111*, 8086−8091.
(9) Bleuzen, A.; Escax, V.; Ferrier, A.; Villain, F.; Verdaguer, M.; Münsch, P.; Itié, J.-P. *Angew. Chem., Int. Ed.* **2004**, *43*, 3728−3731.
(10) Pierloot, K.; Vancoillie, S. *J. Chem. Phys.* **2006**, *125*, 124303.
(11) (a) Reiher, M. *Inorg. Chem.* **2002**, *41*, 6928−6935. (b) Paulsen, H.; Trautwein, A. X. *Top. Curr. Chem.* **2004**, *235*, 197−219.
(12) (a) Suaud, N.; Lepetit, M.-B. *Phys. Rev. B* **2000**, *62*, 402−409. (b) Muñoz, D.; Illas, F.; Moreira, I. de P. R. *Phys. Rev. Lett.* **2000**, *84*, 1579−1582. (c) Hozoi, L.; de Vries, A. H.; Broer, R. *Phys. Rev. B* **2001**, *64*, 165104. (d) Calzado, C. J.; Malrieu, J.-P. *Phys. Rev. B* **2001**, *63*, 214520. (e) Sadoc, A.; de Graaf, C.; Broer, R. *Phys. Rev. B* **2007**, *75*, 165116 (and references therein).

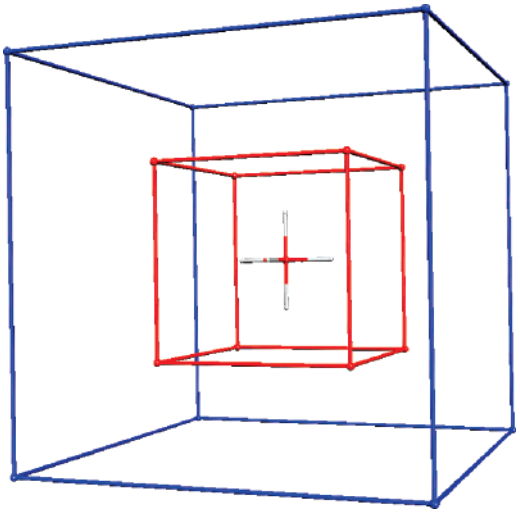

Figure 3. Representation of a $n = 1$ (red) and $n = 2$ (blue) cubic environment. Point charges are not indicated for clarity.

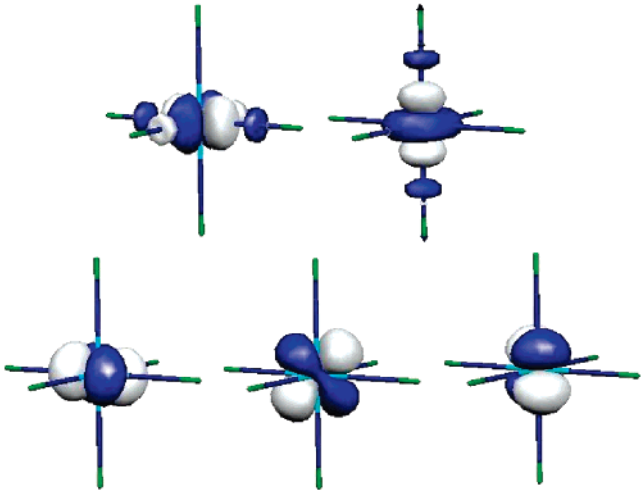

Figure 4. Active orbitals of the $[Fe(NC)_6]^{4-}$ core in the CAS(5,6) calculations. A similar picture holds for the embedded cluster.

field has been clearly demonstrated in solid-state materials,[13] we concentrated on the influence of the Madelung field in the spin transition in terms of bond distance breathings and charge redistributions. Whereas the former are directly known from X-ray experiments, the latter cannot be quantitatively evidenced. Therefore, unrestricted Hartree−Fock periodic calculations were performed using the experimental low-temperature and high-temperature structures to extract the Mulliken charges. Whereas these values are directly evaluated for the iron, chromium, and cesium ions, the charge of the CN group was defined to ensure the crystal neutrality. Thus, each cyano group of the environment was depicted as a single point charge located in the middle of the CN bond. To evaluate the $[Fe(CN)_6]^{4-}$ core electronic structure sensitivity to the Madelung field, environments based on formal charges were also considered. Depending on the number of point charges used to generate the environment, the relevant interaction range was also investigated in this system. Practically, each environment was constructed by symmetrically expanding the crystal along the three lattice vectors around the $[Fe(NC)_6]^{4-}$ core, the iron center crystallographic position being (0, 0, 0). The symmetric construction of the environment is defined by an expansion $\pm n(a/2)$ along each lattice vector (Figure 3). An Evjen's procedure[14] was used to ensure the convergence in the Madelung field. Finally, because disorder has been reported for the cesium atomic positions, different combinations for tetrahedral interstitial sites occupations were considered. As a matter of fact, the local disorder in the cesium ions' positions might be responsible for the spin transition. Let us mention that we concentrated on the filling of the nearest-neighbor tetrahedral positions by cesium ions while the crystallographic positions (1/4, 1/4, 1/4), (−1/4, −1/4, 1/4), (−1/4, 1/4, −1/4), (1/4, −1/4, −1/4) were chosen for the rest of the environment. All of our periodic calculations were carried out with the *CRYSTAL 98* package,[15] using all-electron double-ζ basis sets for iron,[16] chromium,[17] carbon, and nitrogen.[18]

Using those environments, CASSCF calculations were then performed. Along this scheme, one qualitatively introduces in the multireference wave function the leading physical configurations in the different states of interest. As reported previously, the choice of the active space depends not only on the number of open shells on the metal but also on the covalent character of the metal−ligand bonds. Because our main goal was to study the influence of the environment characteristics on the HS−LS energy gap, an active space consisting of six electrons in five valence orbitals (CAS(6,5)) was used in our calculations. Any enlargement of the CAS leaves the additional orbitals either doubly occupied (i.e., inactive) or vacant (i.e., virtual). Finally, to avoid the presence of intruder states, the CASPT2 calculations were performed using an imaginary level shift of 0.2 au.[19] All of our calculations were carried out with the 6.2 version of the *MOLCAS* package[20] including atomic natural orbitals as basis sets for all of the atoms, namely (21s15p10d6f4g) contracted to [5s4p3d1f] for the iron atom[21] and (4s9p4d3f) contracted to [3s2p1d] for the nitrogen and carbon atoms.[22]

Results

1. Gas-Phase Calculations on $[Fe(NC)_6]^{4-}$. Let us first concentrate on the results of the CASSCF/CASPT2 calculations for the $[Fe(NC)_6]^{4-}$ complex in the gas phase. As expected, the active space consists in the mainly 3d iron orbitals (Figure 4). The absence of the environment corresponds to $n = 0$ in Figure 5. In agreement with a low-field versus high-field analysis, the LS equilibrium geometry (i.e., low-temperature phase) favors a LS state over the HS one by ∼2300 cm^{-1} (Table 1). Consistently, the spin states'

(13) (a) Barandiaran, Z.; Seijo, L. *J. Chem. Phys.* **1988**, *89*, 5739−5746. (b) Lepetit, M.-B.; Suaud, N.; Gellé, A.; Robert, V. *J. Chem. Phys.* **2003**, *118*, 3966−3973.
(14) Evjen, H. M. *Phys. Rev.* **1932**, *39*, 675−687.
(15) Saunders, V. R.; Dovesi, R.; Roetti, C.; Causà, M.; Harrison, N. M.; Orlando, R.; Zicovich-Wilson, C. M. *CRYSTAL98*; University of Torino: Torino, Italy, 1998.
(16) (a) Valerio, G.; Catti, M.; Dovesi, R.; Orlando, R. *Phys. Rev. B* **1995**, *52*, 2422−2427. (b) Moreira, I. de P.R.; Dovesi, R.; Roetti, C.; Saunders, V. R.; Orlando, R. *Phys. Rev. B* **2000**, *62*, 7816−7823.
(17) (a) Catti, M.; Sandrone, G.; Valerio, G.; Dovesi, R. *J. Phys. Chem. Solids* **1996**, *57*, 1735−1741. (b) Ruiz, E.; Llunell, M.; Alemany, P. *J. Solid State Chem.* **2003**, *176*, 400−411.
(18) Dovesi, R.; Causa, M.; Orlando, R.; Roetti, C. *J. Chem. Phys.* **1990**, *92*, 7402−7411.
(19) Forsberg, N.; Malmqvist, P.-Å. *Chem. Phys. Lett.* **1997**, *274*, 196−204.
(20) Anderson, K.; Fülscher, M. P.; Karlström, G.; Lindh, R.; Malqvist, P. A.; Olsen, J.; Roos, B.; Sadlej, A. J.; Blomberg, M. R. A.; Siegbahn, P. E. M.; Kello, V.; Noga, J.; Urban, M.; Widmark, P. O. *MOLCAS*, version 6.2; University of Lund: Lund, Sweden, 1998.
(21) Pou-Amerigo, R.; Merchan, M.; Widmark, P.-O.; Roos, B. O. *Theor. Chim. Acta* **1995**, *92*, 149−181.
(22) Widmark, P.-O.; Malmqvist, P.-A.; Roos, B. O. *Theor. Chim. Acta* **1990**, *77*, 291−306.

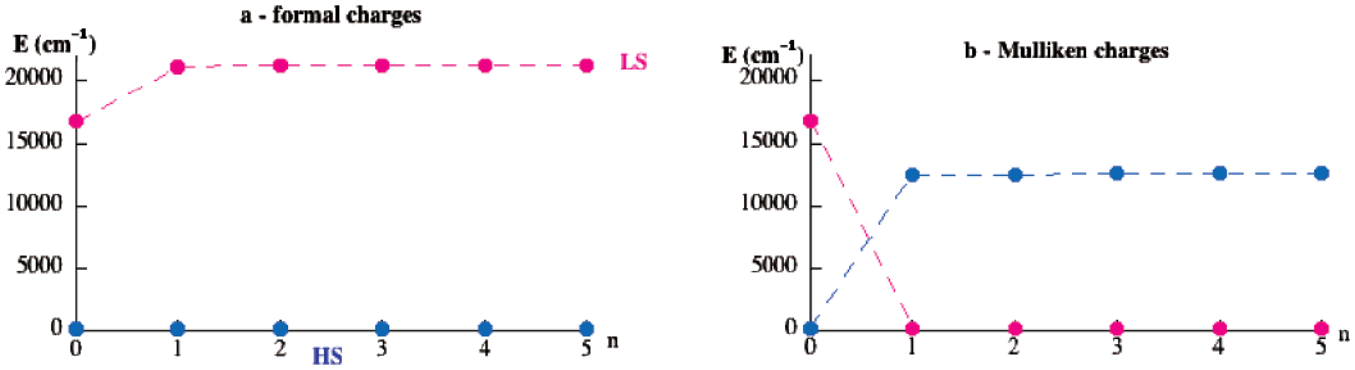

Figure 5. Evolution of the HS/LS splitting with respect to the number n of elementary cells. $n = 0$ corresponds to the gas phase. The dotted lines do not correspond to the physical situation but are added to guide the eye.

Table 1. Energy Differences ($\Delta E = E(^5T_{2g}) - E(^1A_{1g})$, in cm^{-1}) between the HS and LS Spin States Using Different Point Charges Environments[a]

		Franck−Condon	
Point Charges	Non-Franck−Condon	HS core geom.	LS core geom.
-	−16 737	−15 881	+2313
formal	−21 197	−16 835 (−16 943)	+982 (+834)
Mulliken LS	−16 364	−16 359 (−16 428)	+1635 (+1531)
Mulliken HS	−17 916	−16 376 (−16 449)	+1610 (+1523)
Mulliken	+12 547	+12 552	+31 985

[a] The Franck−Condon energy gaps are calculated with the environment geometry corresponding to the same spin state as the core or (in parentheses) to the opposite spin state.

ordering is reversed in the HS equilibrium geometry (i.e., high-temperature phase) whereas the energy splitting is ∼16 000 cm^{-1}. Inspection of the absolute energies in both geometries shows that the non-Franck−Condon spectroscopy displays a HS state lower in energy than the LS state (Table 1 and Figure 5 ($n = 0$)). As reported previously,[5] this observation completely rules out the possibility of observing any spin-transition phenomenon. Indeed, the latter being entropy driven requires a LS ground state.

To investigate the possibility of electron transfer between cations, similar calculations on a dimeric unit [(CN)$_5$Fe−NC−Cr(CN)$_5$]$^{6-}$ were performed. We did not observe the presence of any low-lying electron transfer state Fe^{3+}−Cr^{2+}, which has been identified in the cobalt homologue.[9]

2. Periodic Calculations: Mulliken Versus Formal Charges. The situation may be somewhat different as the Madelung field is turned on. Thus, the next step was to include the crystal environment. These lattice effects were taken into account electrostatically using a Madelung field acting on the [Fe(NC)$_6$]$^{4-}$ complex. Let us mention that the environment is depicted using bare charges without any ab initio embedded model potentials. Because the valence electrons occupy mainly iron 3d orbitals with rather-negligible delocalization tails on the cyano groups (Figure 4), one may assume that orthogonality with the rest of the crystal is reasonably achieved.

To estimate the point-charge values, unrestricted Hartree−Fock periodic calculations were performed on the CsFe[Cr(CN)$_6$] solid using the LS (100 K) and HS (265 K) crystal data reported in the literature.[7] These calculations determine the Mulliken charges in both spin states. Together with the formal charges (+2, +3, +1 for iron, chromium, and cesium, respectively, and −1 for CN), these values were used to construct the purely electrostatic environment around the explicitly ab initio treated [Fe(NC)$_6$]$^{4-}$ core. As seen in Table 2, the Mulliken charges on the chromium and cesium ions and CN groups do not significantly change between the two spin states. This is to be contrasted with electron withdrawal on the iron center as the system undergoes the LS−HS transition. As expected, the occupation of the antibonding e_g set in the HS state removes electron density on the metal. Thus, the Mulliken charge of the latter increases by ∼0.5. In the following, these sets (Table 2) shall be referred to as HS and LS Mulliken charges, respectively.

Table 2. Formal Charges and Computed Mulliken Charges in the LS and HS Crystal Structures

		Fe	Cr	CN	Cs
formal charges		+2.00	+3.00	−1.00	+1.00
Mulliken charges	LT struct.	+1.65	+1.85	−0.725	+0.85
	HT struct.	+2.15	+1.90	−0.80	+0.75

Different problems arise within this strategy. First, what is the minimal size of a fragment creating the embedding potential required to produce the inversion of the energy levels? Besides, the definition of the point charges that must be included in the description of the Madelung potential remains a difficult and not straightforward task. Along the spin-transition phenomenon, it is expected that a given center may be in a specific immediate environment (say LS) originated either by ions holding the same spin states (LS) or by ions which have already transited (thus HS).

3. Embedded [Fe(NC)$_6$]$^{4-}$ Cluster Calculations. To evaluate the influence of the embedding bath, CASPT2 calculations were performed using a different environment of the cubic shape characterized by the expansion $\pm n(a/2)$ of the crystal along each CN bond (Figure 3). As seen in Figure 5, the energy difference between the two states is converged as soon as $n = 2$ (Table S1 in Supporting Information). At this stage, no disorder in the cesium ions' positions was introduced in our calculations. As the whole crystal including the [Fe(NC)$_6$]$^{4-}$ core is expanded, one investigates a non-Franck−Condon spectroscopy of a molecular species immersed in a Madelung environment. Whatever a given set of charges (either formal, high-spin, or low-spin Mulliken charges), the energetics is almost

unaffected as compared to the gas phase (Table 2, lines 2−4). Thus, the breathing of the crystal lattice without any charge reorganization cannot account for the spin-crossover phenomenon.

Let us now examine separately the influence of (i) the lattice breathing and (ii) the charge redistribution accompanying the spin transition. We shall first concentrate on the geometric degree of freedom. Strikingly starting from a high-temperature structure, a HS ground state survives for the frozen $[Fe(NC)_6]^{4-}$ core (i.e., Franck−Condon spectroscopy) as the lattice parameters of the environment are reduced (energy evolution, column 2 of Table 1, values in parentheses). The LS state remains ∼16 000 cm^{-1} above, and the energetics is almost unaffected by the set of charges (less than 1%). A similar conclusion is drawn for the LS ground state (column 3 of Table 1) as an expansion of the lattice is operated. One can conclude that the energetics of a d^6 ion immersed in a frozen-charge matrix is consistent with the Tanabe−Sugano diagram for an isolated complex.

The situation is greatly modified when the electronic redistribution in the covalently bonded lattice is explicitly taken into account. Energies of both states were calculated using the low- and high-temperature crystal structures combined with the calculated HS and LS Mulliken charges. Along this scheme, both degrees of freedom are simultaneously varied. As seen in Table 1, the LS state immersed in a LS environment is stabilized by ∼12 500 cm^{-1} over the HS state in a HS field. Therefore, the charge reorganization plays a dominant role in the creation of prerequisites for the spin-transition phenomenon (crossing in part b of Figure 5). In light of this observation, one may wonder how much the local ligand field $(NC)_6$ competes with the fluctuating Madelung environment. For a long time, the relative contribution of short-range and long-range effects has been discussed in application to cooperativity of molecular spin-transition systems. The priority is usually given to long-range effects, which are considered to be responsible for the spin-transition cooperativity. The coexistence of short-range and long-range interactions of different signs can lead to a two-step spin transition.[23] The calculations of a transiting complex demonstrate the role of cooperativity, which is here accounted by the Madelung field. Interestingly, the simultaneous charge reorganization and lattice contraction greatly stabilizes the LS state of an iron(II) center in a local low ligand field. Indeed, complementary calculations showed that the HS state lies ∼76 000 cm^{-1} higher in energy, a spectroscopy that is rather contrasted with a d^6 Tanabe−Sugano diagram analysis, which favors a HS ground state. Finally, let us note that the charge reorganization without lattice contraction is sufficient to reverse the spin-state order within the same $[Fe(NC)_6]^{4-}$ low field unit (calculated LS/HS gap ∼12 500 cm^{-1}). In light of our analysis of the $CsFe[Cr(CN)_6]$ compound, not only is the leading phenomenon undoubtedly the charge reorganization but the short-range effects seem to dominate over the long-range ones

(23) (a) Romstedt, H.; Spiering, H.; Gütlich, P. *J. Phys. Chem. Solids* **1998**, *59*, 1353−1362. (b) Romstedt, H.; Hauser, A.; Spiering, H. *J. Phys. Chem. Solids* **1998**, *59*, 265−275.

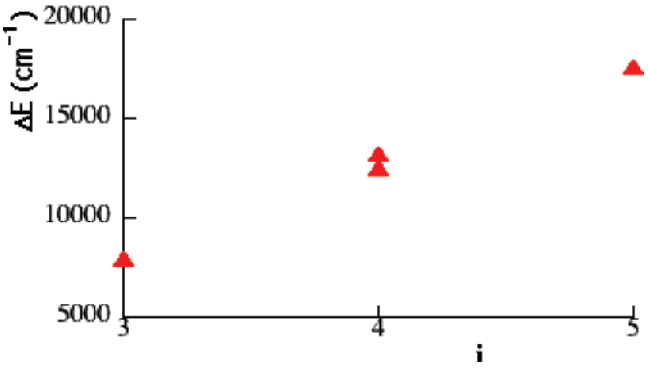

Figure 6. Quintet-singlet energy gap as a function of the number of nearest-neighbor cesium ions. For **i** = 4, the dispersion accounts for the local disorder of the tetrahedral sites' occupation.

because all of our energy differences are rapidly converged with respect to *n* (Table S1 in SI).

4. Alkali Disorder Influence. Let us now examine the importance of the cesium ions' distribution in the energy levels ordering. Starting from a local tetrahedral cesium environment around the iron ion (crystallographic reference position (1/4,1/4,1/4), (−1/4,−1/4,1/4), (−1/4,1/4,−1/4), and (1/4,−1/4,−1/4)), the filling of the nearest tetrahedral sites by cesium cations (Computational Details section) was varied to evaluate the possible influence of disorder on the spin-transition phenomenon. Let us mention that the cesium positions in the rest of the environment were not modified.

As long as the number of nearest-neighbor cesium ions (**i**) remains equal to 4, the energetics is not significantly altered (∼5%) when the cesium ions are moved from the crystallographic reference positions. This is to be contrasted with the disordered situations where the number of nearest cesium ions **i** changes. Interestingly, the larger the number of cesium cations in the nearest environment, the larger the LS state stabilization (Figure 6). Therefore, for this particular system, the solvation of the iron(II) ion in a locally disordered cesium bath may not be sufficient to favor the LS over the HS state. However, as seen in Figure 6, the energetics is very sensitive to the number of nearest cesium cations. Thus, one may wonder whether the spin-transition phenomenon may not be tuned using a different cation.

Conclusions

Our CASPT2 quantum-chemical calculations demonstrate that the crystal matrix of the $CsFe[Cr(CN)_6]$ compound creates conditions for the spin transition of the iron(II) ion, a phenomenon that does not exist for an isolated $Fe(NC)_6$ complex. To properly describe these conditions, one has to include not only structural relaxations but more importantly charge redistributions within the covalently bonded lattice. The importance of both effects distinguishes solid-state systems from mainly considered molecular crystals exhibiting spin transition. However, in some complexes containing the heteroligand $Fe^{II}L(NC)_x$, the spin transition can take place if the ligand L, and possibly the rest of the molecule, if one deals with a polynuclear complex, leads to an overall decrease of the effective ligand field. Probably such effects

are at the origin of the observed spin transitions in tetra-[24] and pentanuclear[25] cyanide clusters. The apparent competition between the ligand field and the fluctuating Madelung environment in the $Fe^{II}(NC)_6$ complex suggests that the spin-transition phenomenon might be expected in other Prussian blue analogues. In the course of our study, the character of cooperativity governing the spin transition has been clarified. It appears that short-order links, including elastic interactions due to the structural relaxation and charge redistributions, produce a mechanism of the spin-transition cooperativity. Interestingly, our calculations suggest that two iron(II) sites holding different spin states can coexist in the 3D system as long as the separation is on the order of two lattice distances. Finally, the spin crossover seems to be sensitive to the local environment generated by the counter cations, a factor which might be experimentally controlled.

Acknowledgment. The authors thank IDRIS for computing facilities.

Supporting Information Available: Table of energy differences between the HS and LS spin states. This material is available free of charge via the Internet at http://pubs.acs.org.

IC701352C

(24) Masayuki, N.; Ui, M.; Yokota, M.; Han, L.; Maeda, A.; Kishida, H.; Okamoto, H.; Oshio, H. *Angew. Chem., Int. Ed.* **2005**, *40*, 6484−6487.

(25) Shatruk, M.; Dragulescu-Andrasi, A.; Chambers, K. E.; Stoian, S. A.; Bominaar, E. L.; Achim, C.; Dunbar, K. R. *J. Am. Chem. Soc.* **2007**, *129*, 6104−6116.